SEMICONDUCTOR DOPING

Movement of atoms or molecules in gaseous, liquid, or solid materials induced by a concentration gradient is called *diffusion*. Diffusion processes are widely encountered in fabrication of semiconductor devices in silicon integrated circuits (ICs) during growth of various layers (epitaxy, oxidation), deposition (evaporation, chemical vapor deposition), etching, and doping.

We will focus on the doping processes, as they are critical steps in p–n junction formation used in all Si devices. These processes take place at high temperatures to facilitate atomic motion in the silicon crystal. The objective of these steps is to create dopants such as acceptors, when impurities from group III of the periodic table are used, or donors, when from group V. By replacing silicon atoms at their substitutional positions in the crystalline lattice, these dopants become ionized and create free charge carriers: holes in p-type Si or electrons in n-type Si. The ionization process requires small energy, of a

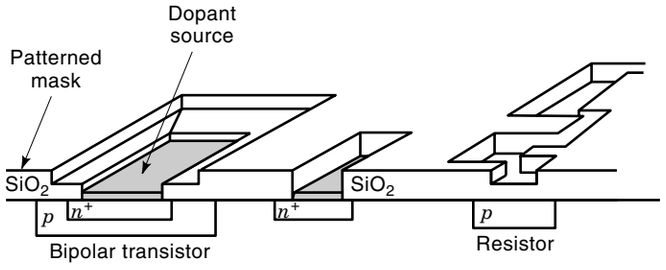

Figure 1. Doping of silicon for fabrication of integrated circuits is performed using a patterned oxide mask. Dopants from groups III and V are used to selectively form p–n junctions in electron devices.

few tenths of electron volts, with acceptor levels that are close to the valence and donors to the conduction band edge, respectively. The dopant and carrier concentrations can be equal at room temperature if silicon is free of crystallographic defects such as dislocations, stacking faults, or precipitates that might trap dopants and/or carriers.

Doping is used to locally introduce impurity atoms into a silicon substrate through a patterned oxide layer that acts as a mask (Fig. 1). Doped layers, in silicon technology, have been traditionally produced by diffusion from gaseous, liquid, or solid dopant sources to form a layer of a pure dopant or of its compounds directly on the substrate. Surface doping creates a concentration gradient at the surface that, at high process temperatures, causes the movement of atoms into the crystal bulk.

The diffusion processes were later replaced by ion implantation, due to its better concentration control. Implantation is followed by thermal annealing for dopant activation and redistribution. Even though ion implantation is used as the source of dopants in IC fabrication, diffusion still plays an important role, since concentration gradients are always present in the doped layers, which cause diffusion during high-temperature annealing.

At present, there is a revived interest in diffusion in very large scale integration (VLSI) and ultra large scale integration (ULSI) ICs, because of submicron sizes of individual devices and consequently more stringent requirements for ultrashallow dopant distributions, even though low-energy ion implantation is being used. New short-time processes are proposed to produce ultrashallow junctions without crystallographic defects in the Si substrate. Among these doping techniques are gas or solid phase diffusion in rapid thermal processing, laser-induced doping from the gas phase, and plasma immersion ion implantation (1). For device fabrication, it is important that these ultrashallow junctions be integrated with the contact layers.

Dopant diffusion occurs by interaction with native point defects (2): silicon interstitials and vacancies that facilitate lattice site exchanges. Analyses of the diffusion processes must include the role of these defects, which if present at excess concentrations, may dominate thermal diffusion. In spite of long experience with diffusion processes in microelectronics and well-documented research data, the task of correctly modeling dopant diffusion for different atoms in various processing conditions is formidable and far from being perfected.

FORMALISM OF DIFFUSION

Mathematically, the diffusion process, for the one-dimensional case, is described by Fick's first law,

$$J = -D\frac{dC(x,\,t)}{dx} \tag{1}$$

which relates the number of diffusing atoms per unit area per unit time, known as the net flux J, with their gradient. The material parameter known as the diffusion coefficient D changes with temperature according to the Arrhenius expression

$$D = D_0 \exp\left(\frac{-E_A}{kT}\right) \tag{2}$$

where D_0 is a constant and E_A is the activation energy, which depends on the matrix (crystalline or noncrystalline Si, oxide, or silicides), impurities, and ambient gas. The diffusion coefficient will be presented later in more detail in the context of atomistic diffusion models of various dopants. The minus sign in Eq. (1) indicates dopant motion from high to low concentrations.

Combining Fick's first law with the continuity equation

$$\frac{\partial C(x,\,t)}{\partial t} = -\frac{\partial J}{\partial x} \tag{3}$$

which links the spatial and time distributions of dopant, we obtain Fick's second law in the most general form for the one-dimensional case:

$$\frac{\partial C(x,\,t)}{\partial t} = \frac{\partial}{\partial x}\left(D\frac{\partial C(x,\,t)}{\partial x}\right) \tag{4}$$

At low doping levels, the diffusion coefficient may be independent of position, thus leading to

$$\frac{\partial C(x,\,t)}{\partial t} = D\frac{\partial^2 C(x,\,t)}{\partial x^2} \tag{5}$$

This second-order differential equation does not have a general solution, but analytical solutions can be obtained by applying correct boundary conditions for specific diffusion processes.

A typical sequence in diffusion processes is composed of two steps: predeposition (prediffusion) and redistribution (rediffusion or drive-in). The first is performed with a constant dopant concentration at the surface (C_s) determined by the solid solubility (3,4) of dopants in Si at diffusion temperature (Fig. 2). The source of dopant here provides an unlimited supply to the Si surface to reach the solubility limits. The boundary conditions for this process, for the one-dimensional case,

$$\begin{aligned} C(x,\,0) &= 0 \\ C(0,\,t) &= C_s \\ C(\infty,\,t) &= 0 \end{aligned} \tag{6}$$

give the solution of Fick's second law in the form of a complementary error function

$$C(x,\,t) = C_s\,\mathrm{erfc}\left(\frac{x}{2\sqrt{Dt}}\right) \tag{7}$$

Here, $\sqrt{Dt}$ is known as the characteristic diffusion length that describes the profile steepness.

An important parameter of the doped layers is the *junction depth,* defined as a distance from the Si surface where the

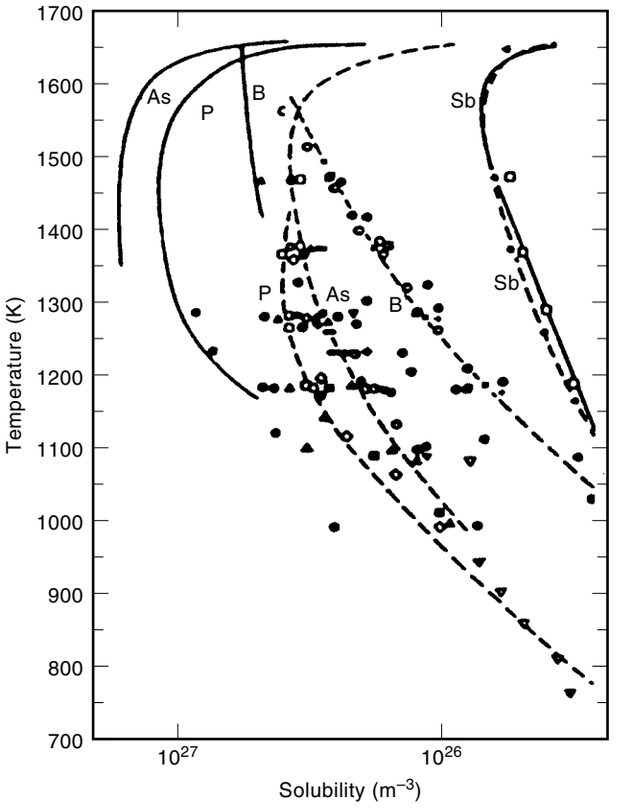

Figure 2. Solid solubility of dopants in silicon as a function of temperature. Dashed lines are calculated using thermodynamic parameters (3).

incoming dopant and substrate concentrations are equal. It can be calculated directly from the prediffusion profiles of observed dopant penetration when $C(x,t) = C_{sub}$ as a function of prediffusion process time:

$$x_j = 2\sqrt{Dt}\,\mathrm{erfc}^{-1}\left(\frac{C_{sub}}{C_s}\right) \tag{8}$$

Linear dependence of the junction depth on $\sqrt{t}$ indicates that the diffusion coefficient D is constant. This is true in *intrinsic* processes, that is, where dopant concentrations are lower than intrinsic carrier concentrations n_i at the diffusion temperature. On the contrary, at high doping levels D depends on impurity concentration. For such *extrinsic* processes, a general form of Fick's second law has to be used [Eq. (4)] with no analytical solution. Each dopant shows a different diffusion enhancement that is determined by its mechanisms of atomic motion via point defects.

Another important parameter in the prediffusion process is the total dose of the introduced dopant, Q_T (cm^{-2}), obtained by profile integration:

$$Q_T(t) = \int_0^\infty C(x, t)\,dx = \frac{2}{\pi}C(0, t)\sqrt{Dt} \tag{9}$$

Q_T increases with the prediffusion time, thus becoming a more efficient dopant source for the subsequent drive-in process. The dose obtained in prediffusion remains constant during rediffusion, since there is no new supply of dopant to the semiconductor surface (limited source diffusion). Distribution of dopant $C(x)$ changes with increasing time, resulting in deeper and less steep profiles. To find $C(x)$ after the redistribution process the following boundary conditions should be used in Fick's second law:

$$\begin{gathered}\frac{dC(0, t)}{dx} = 0 \\ C(\infty, t) = 0 \\ \int_0^\infty C(x, t)\,dz = Q_T\end{gathered} \tag{10}$$

The solution is a Gaussian function:

$$C(x, t) = \frac{Q_T}{\sqrt{\pi Dt}}e^{-x^2/4Dt} \qquad \text{for} \quad t > 0 \tag{11}$$

where D is the diffusion constant of the drive-in process and t is the process duration. The surface concentration

$$C_s = C(0, t) = \frac{Q_T}{\sqrt{\pi Dt}} \tag{12}$$

decreases with time due to the dopant motion, which also increases the junction depth:

$$x_j = \sqrt{4Dt\ln\left(\frac{Q_T}{C_B\sqrt{\pi Dt}}\right)} \tag{13}$$

Distributions of dopants obtained in prediffusion and drive-in processes, respectively, for intrinsic semiconductors are shown in Fig. 3.

Ideal Gaussian distribution may not be appropriate for processes performed for short redistribution times and long predepositions when the ratio of their diffusion lengths is larger than 4. The prediffusion profile cannot be approximated by the step function, and the expression for the profiles after drive-in steps (5) will be described by the Smith function.

At high dopant levels in drive-in steps, similarly to the prediffusion anomalies, due to dependence of the diffusion constant on concentrations, the Gaussian function is not a valid solution of Fick's second law. In these cases dopant profiles are deeper than in the intrinsic diffusion processes. These issues will be discussed later for specific dopants in Si using proposed diffusion mechanisms.

REALIZATION OF THE DIFFUSION PROCESSES

Diffusion processes used for junction fabrication have been designed as a sequence of prediffusion and drive-in. In early technologies, pure dopant layers were used as sources, but they were later abandoned due to problems related to surface damage (pitting) and doping nonuniformity. Next, new sources were introduced as doped oxides ($SiO_2 \cdot B_2O_3$, $SiO_2 \cdot P_2O_5$, etc.) fabricated by growth or deposition processes. Dopant concentrations in these sources were usually high in order to reach the solid solubility limits in Si, and thus to ensure process reproducibility and control of the prediffusion step. Traditionally, various gaseous (PH_3, AsH_3, BCl_3), liquid ($POCl_3$, BBr_3), or solid dopant sources were used. At high temperatures, the doped oxides in reaction with Si released dop-

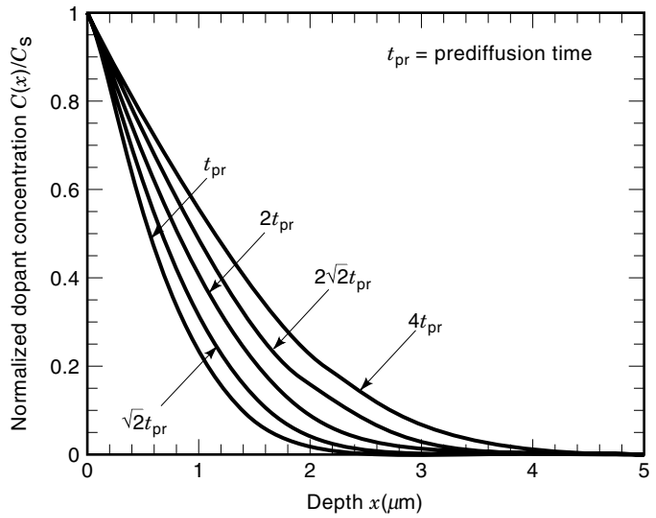

Figure 3. Dopant distributions obtained during diffusion processes at fixed temperatures with varying process time. (a) Prediffusion is described by the erfc function. Increasing process duration causes deeper dopant penetration with the fixed surface concentration determined by the solid solubility. (b) Gaussian distribution is obtained after drive-in processes where limited dopant supply (constant Q_T) results in decreasing concentrations at the surface and larger junction depths for longer processes.

ants available for solid-state diffusion

$$B_2O_3 + \frac{3}{2}Si \rightarrow 2B + \frac{3}{2}SiO_2 \quad (14)$$

$$P_2O_5 + \frac{5}{2}Si \rightarrow 2P + \frac{5}{2}SiO_2 \quad (15)$$

Deposition of B_2O_3 or P_2O_5 on Si was done by their evaporation, which was controlled by the dopant partial pressure via the oxide temperature. Later, these sources were formed in reactions of dopant vapors with oxygen from the ambient gas. Dopant sources were also deposited as spin-on dopants (SODs) such as silicates or siloxides with built-in dopant oxides. Source preparation required spin coating of silicon wafers followed by low-temperature baking to remove organic solvents and form solid doped oxides. SOD sources have been recently reported for a possible alternative technique for ultrashallow-junction formation in ULSI circuits (6). Other dopant sources include solid dopant disks (7) made of compounds (BN with a B_2O_3 layer; bulk SiP_3O_7 or $AlAsO_4$) that decompose at high temperatures to release the dopant oxides and transport them to silicon wafers. A schematic of the prediffusion steps using solid dopant sources for batch processing is shown in Fig. 4.

The drive-in processes were usually realized at higher temperatures, where diffusion coefficients were larger than in prediffusion, so that the Gaussian profiles could be obtained. The requirement of constant dose during redistribution was realized by removal of the dopant source or its deactivation by formation of the SiO_2 layer under the source. At high temperatures, if the surface was not protected after source removal, outdiffusion of dopant to the ambient could cause its substantial loss (8).

The goal of drive-in was to create required dopant profiles and to form a passivating layer for isolation and/or alignment of subsequent doped layers or contacts. Therefore, in the redistribution step, the substrate was either oxidized or else an oxide was deposited and followed by densification to ensure good dielectric and chemical properties. However, oxidation introduces a diffusion anomaly such as enhancement (P and B) and retardation (Sb), as will be discussed later for specific impurities.

In the submicron range of junction depths in VLSI or ULSI circuits, if chemical source diffusion is used for doping, a one-step process is preferred to the sequence of prediffusion and redistribution. One-step diffusion was unacceptable for deeper junctions because the high temperatures necessary to reach the required depths, combined with the solid solubility important for process reproducibility, would have introduced undesirable high dopant concentrations into the doped layers. In addition, lattice deformation and misfit dislocation formation (9) would have resulted from such process conditions.

ATOMIC MODELS OF DIFFUSION

Point Defects

Point defects (2,3,10) that affect dopant diffusion are the vacant sites (vacancies) in the crystal, with concentration C_V; interstitials (i.e., atoms that reside between the host atoms), with concentration C_I; and interstitialcies (i.e., pairs of nonsubstitutional atoms that are placed about one substitutional site). Diffusion (2,11) relies on the probability of defect formation and on the energy of thermally activated dopant atoms. This is described by thermodynamical parameters (the entropy ΔS and enthalpy ΔH) of the formation and the migration of vacancies and interstitials.

The formation of point defects depends on thermal oscillation of the host atoms, which increases with temperature. In a bounded crystal, under thermal equilibrium conditions, there are C_V^* thermally generated vacancies and C_I^* interstitials per unit volume. Their concentrations are not equal, due to their independent migration to the surface and subsequent

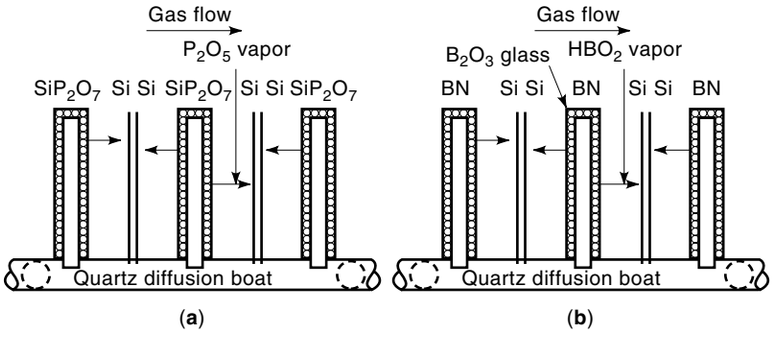

Figure 4. Solid dopant sources used as planar disks that release dopant oxides to be transported in the gas phase to the silicon wafers (7). (a) P source decomposes during the diffusion process, and (b) B source relies on the initial oxidation of BN and subsequent evaporation of B_2O_3.

recombination. The surface can be also a source of point defects from which generated defects can flow to the bulk crystal. This is especially important under nonequilibrium conditions, where populations of vacancies or interstitials are controlled by chemical reactions of Si with the ambient gas, as in Si oxidation and/or nitridation of Si or SiO_2 (oxynitridation); by bulk SiO_2 precipitates (12) caused by oxygen introduced in Czochralski crystal growth; and/or by high dopant concentrations (13), leading in particular to precipitation formation. The V–I recombination process can be very slow due to the energy barrier, so that vacancies and interstitials can exist independently in the crystal.

Vacancies, but not interstitials, were identified experimentally (14) at low temperatures in electron paramagnetic resonance and deep-level transient spectroscopy measurements. At high temperatures, corresponding to the diffusion processes, interstitials have been characterized indirectly from experiments on silicon diffusion (self-diffusion) combined with platinum and gold diffusion results. Arrhenius dependence of their concentration was deduced, with activation energy 3.2 eV. For vacancies, the range of their possible concentrations was also obtained for high temperatures from positron annihilation studies (15).

Point defects can have multiple charge states (2,11) that are important for dopant diffusion and cause its enhancement or retardation. Vacancies' energy levels were identified as 0.57 eV and 0.11 eV below the conduction band for V^- and V^{--}, respectively, and 0.05 eV and 0.13 eV above the valence band for V^+ and V^{++}, respectively. Interstitial levels were also found (16). Concentrations of the various charged defect states, except for neutrals, depend on doping levels via the Fermi level difference in the doped layer (E_s) and in the intrinsic semiconductor (E_f^i)

$$\frac{C_{x^-}}{(C_{x^-})^i} = \exp\left(\frac{E_f - E_f^i}{kT}\right) \tag{16}$$

Using relations between carriers in semiconductors and their Fermi levels, concentrations of charged defects can be obtained:

$$\frac{C_{x^-}}{(C_{x^-})^i} = \frac{n}{n_i}, \qquad \frac{C_{x^{--}}}{(C_{x^{--}})^i} = \left(\frac{n}{n_i}\right)^2 \tag{17}$$

$$\frac{C_{x^+}}{(C_{x^+})^i} = \frac{p}{n_i}, \qquad \frac{C_{x^{++}}}{(C_{x^{++}})^i} = \left(\frac{p}{n_i}\right)^2 \tag{18}$$

Negatively charged defects increase with doping in *n*-type silicon and decrease in *p*-type silicon, while positively charged defects behave in the opposite manner.

Diffusion Mechanisms

Dopant atoms in the crystal during diffusion interact with point defects as follows:

$$A + V \rightleftharpoons AV \tag{19}$$

$$A + I \rightleftharpoons AI \tag{20}$$

$$A + I \rightleftharpoons A_i \tag{21}$$

$$A \rightleftharpoons A_i + V \tag{22}$$

and describe possible diffusion mechanisms of dopants as illustrated in Fig. 5.

The vacancy mechanism [Fig. 5(a)], where the atom interacts with a vacancy and moves as a complex [Eq. (19)] rather than by a single exchange process, was widely accepted in early studies of Si self-diffusion. This diffusion mechanism applied to dopants would result, however, in the same diffu-

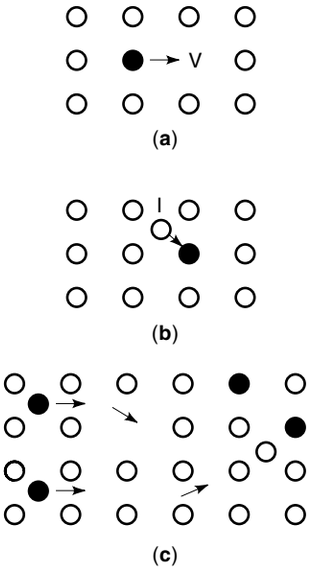

Figure 5. Atom diffusion processes include (a) vacancy mechanism, (b) interstitialcy mechanism, which involves knockout of the host atoms, and (c) interstitial mechanism.

sion coefficients as for Si during self-diffusion. Since experimentally observed diffusivities of dopants are larger and their activation energies are smaller than those for Si, dopant–defect pairs were postulated (2). It is important to notice that the simple Coulombic attraction between the dopant and defect does not explain the differences in activation energies, and a non-Coulombic potential interaction beyond the third nearest neighbor sites must be present if vacancy models are to be used. The vacancy model, adapted for various dopants, is still used in some process simulators.

The interstitialcy mechanism occurs when incoming atoms create interstitials, which enhance the dopant motion [Fig. 5(b)], before entering a substitutional position. In the interstitial mechanism atoms move between host lattice sites [Fig. 5(c)]. In both cases, increasing concentrations of point defects leads to diffusion enhancement. The diffusing atom–interstitial (AI) defects do not dissociate, in contrast with atom–vacancy (AV) partial dissociation. These models (kickout) were dismissed earlier on account of estimations that silicon interstitial formation requires very high energy. However, Seeger and Chick (17) showed that the vacancy mechanism is prevalent at low temperatures while interstitial-assisted diffusion takes place at high temperatures. There is now overwhelming evidence that interstitials play a crucial role in diffusion of many dopants.

To create an electrically active dopant (i.e., an atom in the substitutional position), the dopant–defect complex has to split into the substitutional atom and defect. That contributes to the excess vacancies or interstitials induced by dopant diffusion. The supersaturation of point defects obviates the requirement for additional effects, such as the growth of precipitates (e.g. SiP), which form at high concentrations and release interstitials from PI pairs.

Both the kickout and vacancy mechanisms [Eqs. (20) and (21)] show formation of dopant–defect complexes that control dopant motion and result in different diffusivities for various dopants. Discussion of specific diffusion mechanisms for various dopants will be presented later.

Equilibrium Conditions

Intrinsic Semiconductors. Migration of defects and dopant–defect complexes depend on the defect type and charges (2,11,18). For instance, interstitials are fast-moving species even at low temperatures (4.2 K), so that even their experimental identification is difficult. Therefore, the role of point defects should be included in the dopant flux. For equilibrium conditions, at low concentration, the transport of dopant is described by the following expression (2):

$$-J_A = d_{AV}\frac{\partial C_{AV}}{\partial x} + d_{AI}\frac{\partial C_{AI}}{\partial x} \tag{23}$$

where d_{AV} and d_{AI} are the diffusivities of dopant-atom–vacancy and dopant–interstitial defects, respectively. Local equilibrium allows us to obtain the flux of dopants as

$$J_A = -D_A^*\frac{\partial C_A}{\partial x} \tag{24}$$

where $D_A^* = D_{AV}^* + D_{AI}^*$ is the measured diffusivity, which depends on defect concentrations and diffusivities:

$$D_{AV}^* = d_{AV}\frac{C_{AV}}{C_A} \quad \text{and} \quad D_{AI}^* = d_{AI}\frac{C_{AI}}{C_A} \tag{25}$$

Each term of the diffusion constant, for every dopant, displays Arrhenius behavior with a different activation energy. The change of C_A with time, as occurs during diffusion, can be calculated directly from the diffusion mechanisms for each dopant–defect reaction, as summarized by Eqs. (19) to (23), and results simply in Fick's second law:

$$\frac{\partial C_A}{\partial t} = D_A^*\frac{\partial^2 C_A}{\partial x^2} \tag{26}$$

with the diffusion constant as in Eq. (24). This is valid in intrinsic semiconductors under quasiequilibrium conditions. It does not need or allow the specification of diffusion mechanisms for the dopant. However, under nonequilibrium conditions, where excess defect concentrations are generated at the surface or in the bulk crystal, the types of point defects and their concentrations have to be specifically known to describe the diffusion process.

Extrinsic Semiconductors. At high dopant concentrations, point defect populations change with the Fermi level [Eq. (16)] and result in modification of the diffusivities responsible for transport of dopant–defect complexes. Fick's second law [Eq. (26)] has to be revised to include dependence of the diffusivity on dopant concentration:

$$\frac{\partial C_A}{\partial t} = \frac{\partial}{\partial x}\left(D_A^*\frac{\partial C_A}{\partial x}\right) \tag{27}$$

where (2,19)

$$D_A^* = h\left[D_{A+X^0}^i + D_{A+X^-}^i\frac{n}{n_i} + D_{A+X^{--}}^i\left(\frac{n}{n_i}\right)^2\right] \tag{28}$$

with

$$h \equiv 1 + \frac{C_{A^+}}{n_i}\left[\left(\frac{C_{A^+}}{n_i}\right)^2 + 1\right]^{-1/2} \tag{29}$$

which acts to additionally enhance the diffusivity of dopants at high concentration levels. The coefficient h is determined by ionized dopants, not by the dopant–defect complexes, since they are considered to be at low concentrations compared to the dopants. Because it represents the effect of electric field, it produces drift of charged defect–dopant complexes. For low dopant concentrations its role disappears, that is, $h = 1$.

Diffusion of dopants into extrinsic but uniformly doped semiconductors does not experience any enhancement due to the electric field, but only due to the defect density change. If the indiffusing dopant is the same as that in the substrate, its diffusion will be enhanced, while for other atoms it may be retarded. Experiments that show slower diffusion of P and Sb in highly doped p-type Si and of B in P-doped silicon were explained (20) by dopant pairing (As–P, Sb–B, etc.), which may slow down the motion of impurity atoms.

Nonequilibrium Conditions

Information about the diffusion mechanisms including vacancy and interstitial contributions can be deduced from nonequilibrium processes. Here, point defects, that are generated at the Si surface and recombine both in the bulk and on the surface are of special interest in the fabrication of integrated circuits.

Generation of interstitials is linked to the oxidation process where interstitials are released to alleviate the stress induced by large (about a factor of two) volume mismatch between the formed SiO_2 layer and the consumed silicon. Their agglomeration on nucleation sites results in the formation of oxidation-induced stacking faults (OISF) (9). Information about the OISFs' growth can be combined with enhancement or retardation of diffusion, called oxidation-enhanced diffusion (OED) and oxidation-retarded diffusion (ORD). The first effect points at the interstitial diffusion mechanism; the second one, at the vacancy-assisted mechanism.

Generation of vacancies occurs during nitridation of the silicon substrate as indicated by the shrinkage of OISFs (21). Dopants that show diffusion enhancement in these conditions move by the vacancy-assisted mechanism, while those that are retarded diffuse by interstitial defects.

Under nonequilibrium conditions but in steady state (as in slow thermal processes), the mass action law describes the point defect population as

$$C_V C_I = C_V^* C_I^* \tag{30}$$

indicating that the increasing concentration of interstitials causes depletion in vacancies due to increased recombination between I and V (the asterisk denotes equilibrium). More accurately, if the flux of vacancies that come from the surface to compensate for their undersaturation is included, then $C_V C_I > C_V^* C_I^*$ and shows that undersaturation of vacancies at the surface is smaller than in the bulk, i.e., the surface becomes a source of vacancies (2).

Insight into the I and V concentrations comes from the continuity equations, which combine concentration changes in time and space as well as generation and recombination reactions. The excess concentration of interstitials, $\Delta C_I = C_I - C_I^*$, becomes $\Delta C_I = g_I/\sigma_I$ where g_I is the generation rate related to the oxidation rate and σ_I describes the surface loss due to recombination. Loss of I at the surface can also result from capture by kinks present at the Si surface. This effect will be seen in effects of the Si orientation in OED experiments.

Recombination of generated V and I in the bulk can occur at the defect sites and is limited by the energy barrier. Enhancement of interstitial loss can be due to trapping by dopants or contaminants, such as C, that may be present in the crystal. The action of carbon is related to interstitial suppression via formation of highly mobile CI pairs. This is considered beneficial for combating B diffusion enhancement and may be included in the processing by addition of C via ion implantation (22,23). C diffuses by the kickout mechanism and does not generate nonequilibrium defects.

Of the nonequilibrium processes, especially interesting are transient effects in diffusion, where the limited diffusivity of defects results in a sharply nonuniform distribution of dopant.

Low Dopant Concentrations. At low doping levels under nonequilibrium conditions the diffusion constants in Fick's second law depend on temperature only, not on concentrations. The values of diffusivities for various dopants are determined by defects [see Eqs. (25) and (26)]. By defining the fractional interstitial component (24) at thermal equilibrium,

$$f_{AI} = \frac{D_{AI}^*}{D_{AI}^* + D_{AV}^*} \tag{31}$$

we can analyze diffusivity differences ΔD_A between nonequilibrium and equilibrium conditions, since f_{AI} appears in the measured diffusion constant

$$D_A = D_A^* \left((1 - f_{AI}) \frac{C_V}{C_V^*} + f_{AI} \frac{C_I}{C_I^*} \right) \tag{32}$$

The direct relation between diffusion enhancement (ΔD_A) and excess interstitials (ΔC_I) gives an estimation of the diffusion enhancement (for large f_{AI}) or retardation (for small f_{AI}) caused by these defects. Vacancy injection results in retardation (Δ_R) or enhancement (Δ_E) of the diffusion constants for large and small f_{AI}, respectively.

By measuring Δ_E and Δ_R for two different dopants under identical process conditions, a bound on f_{AI} was found as $f_{AI} > 1 - \Delta_R/\Delta_E$ for different dopants $f_{SbI} < f_{AsI} < f_{PI} \approx f_{BI}$. It has been recently shown that the values of the interstitional factors can be calculated without any other assumptions than local equilibrium (25) and that dopants can either diffuse by interstitials (e.g. boron and phosphorus), so that $f_{AI} = 1$, or by vacancies (e.g. Sb), so that $f_{AI} = 0$.

High Dopant Concentrations. An increase of defect populations that control a given doping mechanism results in enhanced diffusion, but the magnitude of the enhancement depends on the fractional interstitial (vacancy) factor. This will be discussed in the context of the oxidation and nitridation processes.

DIFFUSION OF IMPURITIES

The fractional interstitial contribution has been a subject of controversy for various dopants and Si diffusion. Self-diffusion shows Arrhenius behavior with an activation energy of about 5 eV, which is about 1 eV larger than that of dopant diffusion, while the diffusivity for Si is smaller than those of dopants. All diffusion mechanisms (vacancy, interstitial–interstitialcy, and dual) have been proposed for self-diffusion (see discussion in Ref. 2).

The diffusion mechanism of all dopants used in semiconductor devices (B, P, As, and Sb) was at first considered to be mediated by vacancies. Many such models (2,11,26) developed for process simulation (27), despite fundamental differences, show a good match with experimentally obtained profiles. Presently, for several dopants (P, B, As) used in the Si technology, there is a consensus that a dual mechanism that involves both vacancies and interstitials is responsible for atomic diffusion. The contributions of each mechanism vary for different dopants with their concentrations, process temperature and ambient gas. However, these issues are still controversial, as the problems related to reaction–diffusion phe-

nomena are extraordinarily complicated and thus not always sufficiently well described.

Phosphorus diffusion proceeds as predicted by Fick's law under intrinsic conditions. However, at heavy doping levels it is slow in the range of high dopant concentrations, with incomplete dopant activation and a plateau region ("kink") of carrier concentrations. High dopant concentrations can cause strain that can lead to misfit dislocation formation. This region is followed by a tail indicating enhanced diffusion. Early models assumed vacancy assisted diffusion (28) where a complex of P^+V^{--}, and to the lesser extent P^+V^x and P^+V^{-3}, was responsible for slow diffusion, while fast diffusion was due to vacancy generation due to the splitting of P^+V^-. This model has been successfully used to simulate phosphorus diffusion profiles at high concentrations (Fig. 6).

However, it is now widely accepted that P diffusion occurs via interstitial mechanisms, in view of the evidence provided by the OISF growth facilitated by high P concentrations (13). Phosphorus is believed to inject interstitials. It enhances diffusion of dopants (B, P, As) in remote layers placed beneath it (buried layers) (29). On the other hand, it retards Sb diffusion in buried layers, but may also enhance it in the same region (13). The last observation may indicate that there is a vacancy component in the P diffusion as well and/or that Sb can have an interstitial component.

Boron, as a negatively charged acceptor, was linked to positively charged vacancies, and the postulated diffusion was based on migration of these extrinsic defect pairs. For boron, the vacancy models used B^-V^+ pairs as a dominating diffusant. Boron diffusion depends on substrate concentrations and can be significantly reduced in highly doped *n*-type material. In addition to proposed pairs with vacancies, it can form pairs with other point defects such as contaminants (3,30) (Fe and Cr) in the Si crystal. Diffusion of boron is also affected by hydrogen (31), which enhances its diffusion in oxide and can also result in compensation of carries in the Si substrate.

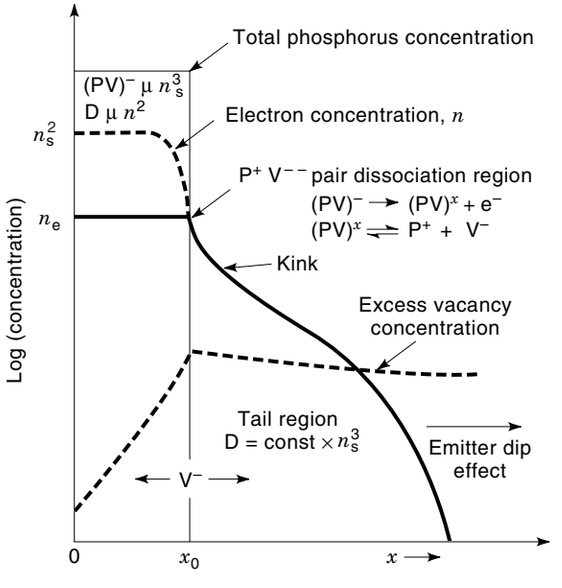

Figure 6. An early model of P diffusion (28) included vacancies and their complexes as the main point defects. Enhancement of diffusion observed experimentally at high dopant concentrations and resulting in the tail formation was explained by splitting of the defect complexes.

Evidence that interstitials are important in B diffusion was provided by experimental results on the OISF growth enhanced by high phosphorus concentrations and on enhancement of B by P diffusion both in buried layers and in bipolar transistors (32) (the pushout effect). In addition, gettering experiments (33) and OED clearly indicated that the same type of point defects (i.e. silicon interstitials) were involved in diffusion of B. However, differences as to the magnitude of the particular mechanism contribution (3,11) for these dopants still exist, with f_{AI} being found as low as 0.17 and as high as 0.99. Recent theoretical expectations, based on the assumption of local equilibrium of point defects only, supported by experimental results, indicate that diffusion of substitutional dopants in Si should follow either a pure vacancy or a pure interstitialcy mechanism (25).

Arsenic is known to diffuse by a dual mechanism, where both vacancies and interstitial play the role (2). Arsenic shows some enhancement of diffusion by oxidation but also by nitridation. At high concentrations in prediffusion processes, the diffusivity increases and dopant profiles do not follow the erfc function. In addition, arsenic can form clusters during diffusion such as VAs_2 (2,19), which decreases the flux of moving complexes and reverses dopant activation. As the result of defect formation, carrier concentrations in heavily arsenic-doped silicon are smaller than the total concentrations of As atoms. The effect of dopant deactivation (34) is more pronounced at low temperatures, where VAs_4 is the dominating defect, than at higher temperatures, where VAs_3Si and VAs_2Si_2 are formed.

Antimony is modeled as a vacancy-assisted diffusion (24,35). Several experiments show an increase in Sb diffusion rates during vacancy generation. Interestingly, high P concentrations also enhance diffusion of Sb (36), even though there is a clear evidence that P induces interstitial generation. That indicates that high concentrations of P, because of the Fermi-level shift to the conduction band, may also cause vacancy generation within the P-doped layer; this is not in contradiction to vacancy undersaturation observed below this layer.

Diffusion of *metallic impurities,* such as gold, is believed to be facilitated by interstitials. Their solid solubility in Si is low for interstitial atoms and high for substitutionals, while their diffusivities are high for interstitial and low for the substitutional motion. An accepted mechanism of gold diffusion is the kickout process, which is linked to the interstitial diffusion processes. Here, silicon interstitials have to be effectively transported away from the substitutional sites of the dopants.

THE ROLE OF OXIDATION AND NITRIDATION DURING DIFFUSION

When diffusion of dopants occurs during oxidation, the growth of oxide results in silicon consumption and therefore creates moving boundary conditions (5). At the $Si–SiO_2$ interface dopants pile up on either the silicon or the oxide side (37) because of interface segregation, thus creating concentration gradients. For the B-doped layers this leads to dopant depletion below the oxide, where the profiles suggest dopant loss due to outdiffusion.

Oxidation leads to nonequilibrium concentrations of point defects and thus induces OED or ORD of various dopants, but provides important information about atomic mechanism of diffusion. For impurities that diffuse with a large interstitialcy component, such as P or B, the diffusion enhancement caused by excess interstitials is very significant. For arsenic, because of its dual (vacancy and interstitial) diffusion mechanism, the increase is smaller. On the other hand, Sb is retarded by oxidation except for an enhancement for very short oxidation times before undersaturation of vacancies is reached; this may indicate some interstitial component in the Sb diffusion mechanism (24).

The influence of oxidation on dopant diffusion will be therefore included in the diffusion equations (38) by modifying the diffusion coefficient D to

$$D_{ox} = D_I \frac{C_I}{C_I^*} + D_V \frac{C_V}{C_V^*} \tag{33}$$

The enhancement of diffusion coefficient due to oxidation (Δ_{ox}) is related to the fractional interstitial contribution $f_{AI} = D_{AI}^*/D_A^*$ by

$$\Delta_{ox} = \frac{(2f_{AI} + f_{AI}S_I - 1)S_I}{1 + S_I} \tag{34}$$

where $S_I = (C_I - C_I^*)/C_I^*$ is the supersaturation ratio for interstitials

The OED of various dopants depends on their concentration, thus confirming that the role of point defects is critical in diffusion processes. Increasing dopant concentrations decreases the OED effect of phosphorus and boron (16). The vacancy generation larger background interstitial concentrations, and/or recombination rates between vacancies and interstitials, can be responsible for this effect, as seen in the P and Sb diffusion experiments mentioned earlier.

OED decreases with increasing temperature, indicating that the supersaturation of interstitials decreases with T, thus providing information on behavior of the interstitional factor f_{AI}. It also shows sublinear dependence on the oxidation rate through the generation rate of interstitials (2).

Oxynitridation, the nitridation of SiO_2, injects silicon interstitials, thus enhancing P diffusion (35). Figure 7 shows enhancement of diffusion coefficients due to oxidation for B, P, and As (39). Nitridation, by injecting vacancies, retards P and B diffusion but enhances Sb diffusion (40).

Information about dopant diffusion is frequently obtained in complementary experiments consisting of ambient-gas studies combined with investigation of the mask pattern's role in point defect generation, migration, and recombination.

THE ROLE OF SUBSTRATE ORIENTATION IN DIFFUSION

Diffusion processes are affected by the concentrations of point defects, but, since there is no clear evidence that their concentrations change in various crystallographic directions, the lateral and in-depth diffusions should be comparable. Experimentally observed differences (41) may appear as orientation-dependent diffusion but in fact be due to point defect generation and recombination at the surface, determined by properties of silicon and passivating masks during oxidation or nitridation (42). Consequently, for silicon with patterned oxide structures, dopant diffusion in the horizontal direction can be retarded by surface recombination, thus resulting in lateral diffusion that may be up to 85% of the vertical diffusion for intrinsic processes, and up to 70% for extrinsic.

However, there is a difference in the diffusion into crystals of different orientations during oxidation or nitridation processes. By generating point defects such as interstitials or vacancies, enhancement or retardation, respectively, can be dependent on the crystallographic orientation. Specifically, for mainly interstitialcy diffusion processes (B and P), larger enhancement is observed for (100) than for (111) planes (19). This is in spite of the larger generation of interstitials on (111) than on (100) planes, as evidenced by faster rates of the oxidation processes for (111) than for (100) planes. ORD was observed for boron (43) and phosphorus (44) doping, and OED for antimony doping, in (111) Si in long-time processes, thus indicating injection of vacancies. However, stronger recombination of these point defects at the silicon (111) surface may be responsible for the smaller OED effect than for (100) due to the presence of surface kinks, which capture silicon interstitials.

DIFFUSION IN POLYCRYSTALLINE AND AMORPHOUS SILICON

Dopant diffusion in a polycrystalline matrix, such as polycrystalline Si (polysilicon), is much faster than in a single crystal

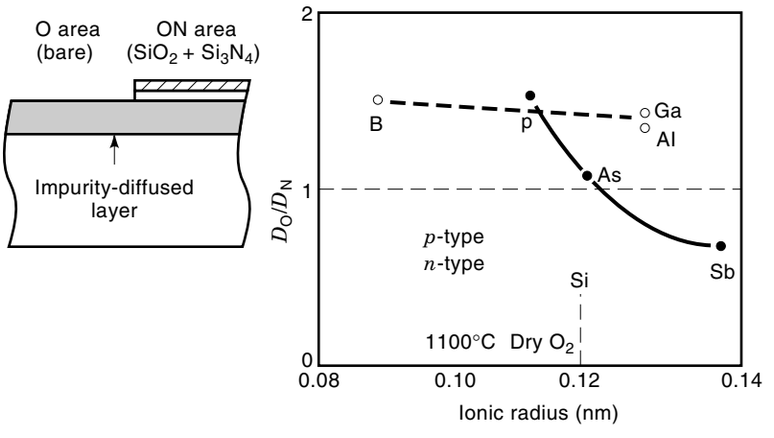

Figure 7. Oxidation-enhanced or -retarded diffusion for various dopants in silicon is related to generation of silicon interstitials (38). P and B show much stronger enhancement than As, thus indicating their interstitial mechanism as opposed to As, which diffuses by a dual vacancy–interstitial mechanism. Sb shows retardation of diffusion related to its vacancy mechanism.

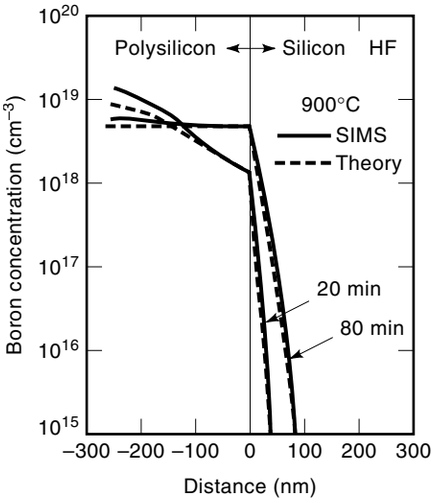

Figure 8. Diffusion of dopants (46) in polysilicon and crystalline silicon as a function of temperature. The faster diffusion in polysilicon is due to the grain boundary migration. Differences between the diffusion constants in poly-Si and c-Si decrease with increasing temperatures because of the grain growth.

due to the presence of grain boundaries acting as diffusion pipelines (45). Similarly enhanced diffusion is observed along dislocation lines in a Si crystal. This increase of diffusion coefficients can be as much as a few orders of magnitude. Diffusion occurs also within the grains, with the same rate as in crystalline Si. The difference in diffusivities between single crystal and polycrystalline Si decreases with increasing temperature because of grain growth, which results in a smaller contribution of grain boundary diffusion. Segregation of dopant into the grain boundaries takes place for P and As but not for B. Fast diffusion in the polycrystalline silicon, and significantly less in amorphous silicon, as compared to the single crystal, has led to wide application of these materials in device fabrication (46) (Fig. 8), where high dopant concentrations and their uniform distributions are required. The doping uniformity of polysilicon can be readily obtained even within thick layers such as gate electrodes in MOS transistors and raised junctions, which facilitate silicide contact formation without degradation related to silicon bulk consumption, in scaled-down devices. These doped polycrystalline or amorphous Si layers act as unlimited dopant sources during diffusion processes. However, because of fast diffusion, dopant loss, especially significant for As, occurs due to outdiffusion to the gas ambient if a capping layer is not used.

MASKING PROPERTIES OF OXIDES

Diffusion of dopants through SiO_2 layers is very important in device fabrication. Slow dopant motion through an oxide mask allows for selective silicon doping within desired device regions. Similarly to the diffusion of various dopants in silicon, diffusion in the oxide also depends on the dopant type and oxide structure.

A two-layer matrix composed of oxide and silicon has to be considered when solving Fick's second law of diffusion (5). Since the diffusion coefficients are not the same in these two materials, and there is discontinuity at the SiO_2–Si interface, two forms of Fick's second law have to be used, one for each material, with boundary conditions that include oxide thickness and segregation (m) at the interface (37):

$$C_{si}(0, t) = mC_{ox}(0, t) \tag{35}$$

Examples of dopant segregation at the SiO_2–Si interface are shown in Fig. 9 for various dopants in various ambient gases. This segregation depends on the dopant type, ambient gas during diffusion, and temperature. Incorporation of the dopant into SiO_2 changes the composition and properties of the glass. The oxide acquires less of a dense structure and at high temperatures shows a lower viscosity that facilitates its flow (47). For boron, the segregation leaves the silicon surface depleted, and dopant accumulation takes place in the oxide during oxidation.

Small thickness of the oxide increases the diffusivity of B because of a Si-rich structure in the transition layer, which, for thin oxides, constitutes a significant part of it (48). The ambient gas also plays an important role in dopant diffusion though oxides (35,49). The usual slow diffusivity of boron in the oxide can be substantially enhanced by fluorine and hydrogen. Interestingly, hydrogen, while itself diffusing very rapidly, also enhances diffusion of B in silicon (31). It causes boron compensation by hydrogen–dopant pair formation, re-

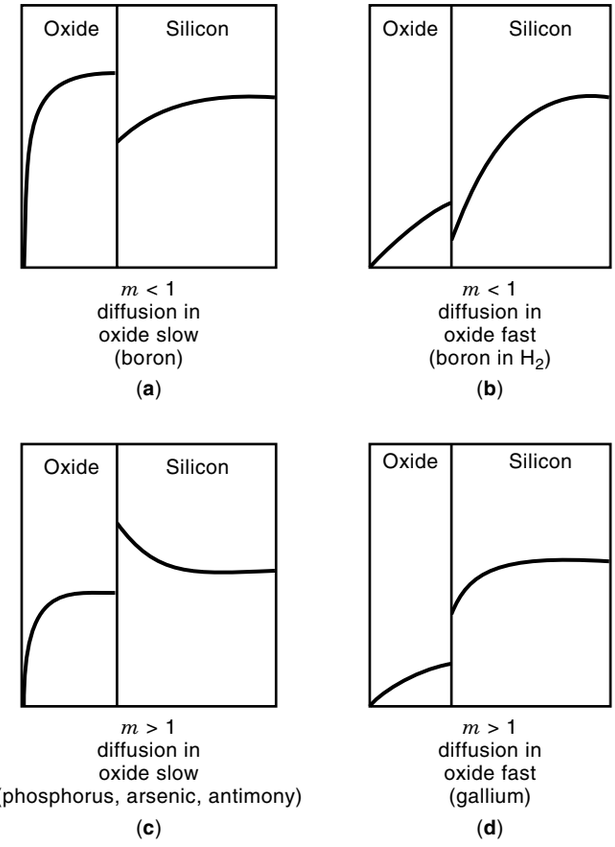

Figure 9. Segregation of various dopants at the interface of SiO_2 and Si during oxidation of a doped semiconductor (37). Fast diffusion of Ga in SiO_2 makes this dopant not useful in silicon technology that requires good oxide masking.

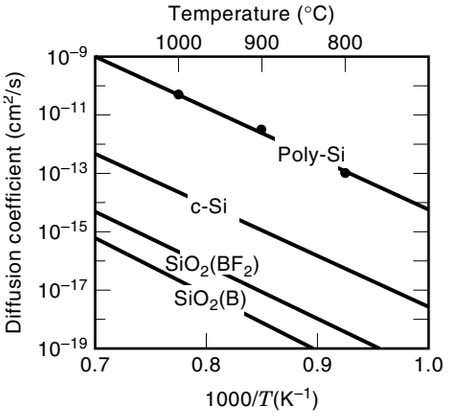

Figure 10. Comparison between the diffusion constants in poly-Si, c-Si, and oxide as a function of temperature (46). Diffusion rates in the oxide are the smallest, but depend on the dopant type.

sulting in an increase of resistivity via reduction of hole concentrations.

For phosphorus, segregation at the SiO_2–Si interface increases the dopant concentration at the silicon surface while the oxide side becomes depleted (50). A similar pileup effect is observed for arsenic and antimony.

Enhancement of diffusivity in the oxide in the presence of high dopant concentrations can be also observed in the oxidation of silicon. This process depends on oxygen diffusion through the growing SiO_2 to the Si surface. Larger oxidation rates on heavily B-doped substrates than on undoped Si are related to larger oxygen diffusivity in the oxide that contains boron, from the doped substrate consumption, than in the undoped SiO_2.

There are a number of species that are considered fast diffusers in silicon dioxide: H_2, OH, H_2O, alkali metals (Na, K), and Ga. This fast diffusion of Ga hinders its masking by the oxide and excludes its potential application as a dopant in Si device fabrication. A comparison between the diffusion constants in poly-Si, c-Si, and oxide is shown in Fig. 10.

DOPANT DIFFUSION IN SILICIDES

Diffusion processes also occur during the formation of silicide used for self-aligned contact layers and formed in reaction of a metal with oxide-patterned Si. Depending on the type of metal and process conditions, either silicon or metal can be the main diffuser (51). A reaction between metals and silicon can result in generation of point defects and therefore can affect dopant diffusion present in a doped layer below the contact. Experiments showed enhancement of Sb and retardation of B diffusion, respectively in superlattice structures where $TiSi_2$ formation was an accompanying process. That indicates generation of vacancies during titanium silicidation. Other observations of the enhancement of Sb diffusion in a buried layer, reported during $PdSi_2$ (52) and TaSi (53) formation, indicated vacancy generation. It is, however, possible (27) that a stress gradient was an additional reason for the enhancement, since B and Ga experienced similar effects. It seems likely that information about process kinetics of dopant diffusion obtained from nonequilibrium conditions (oxidation, nitridation) can be greatly improved by incorporation of silicidation studies into diffusion experiments.

Diffusion of dopants in silicides can be used to integrate the processes of junction and contact formation. Here, a *silicide as diffusion source* (SADS) (54) is implemented to outdiffuse the dopants from the silicide or metal layers to form junctions. Since the structure of silicides usually is not crystalline, the diffusion of dopants is fast along grain boundaries. Diffusion from some silicides has yet another aspect, related to metal–dopant compound formation (55), that can limit dopant outdiffusion from the silicide layer into silicon. This is indeed observed in SADS, where one type of the dopant (*n*- or *p*-type) diffuses fast and the other one slowly, due to metal–dopant compound formation. On the other hand, this process can be used to create a diffusion barrier (TiB_2) that may prevent junction degradation by hindering the silicidation process (56).

STRESS AND DIFFUSION

The influence of stress in a semiconductor, either applied externally or induced by processing such as oxide or nitride growth, is well documented. The analysis of dopant diffusion under stress conditions has to include the effect of stress on the generation and migration of point defects. Interesting reviews (27,57) refer to many aspects of lattice deformation and its effects on various silicon processings. Change in the lattice parameters, such as that induced by high dopant concentrations that causes energy bandgap narrowing, results in decreased diffusivity (43). Doping of trench structures results in similar nonuniformities of junction depths to those of oxides thermally grown (58).

CHARACTERIZATION OF DOPED LAYERS

Doping characterization is based on electrical, physical, and chemical measurements. Active dopants present in diffused layers contribute to the resistance R_s (Ω/square), known as the sheet resistance:

$$R_s = \frac{1}{q}\left(\int_0^{x_j} \mu(x)n(x)\,dx\right)^{-1} \tag{36}$$

where $n(x)$ is the concentration of carriers and $\mu(x)$ is the mobility. Sheet resistance allows for easy design of resistors in ICs where they are built in the same diffusion layer. Since the sheet resistance represents the value for a square resistor, by selecting length (L) and width (W) values for the oxide mask during diffusion, the number of squares, $N = L/W$, can be utilized to give the actual resistance,

$$R = NR_s \tag{37}$$

Values of R_s can be calculated from the dopant profile if the carrier mobility is determined only by dopant concentration without any deterioration caused by process-induced defects. Sheet resistances combined with junction depths are available as plots for erfc and Gaussian dopant distributions for various substrate concentrations. However, for extrinsic diffusion processes, where diffusion is enhanced by high dopant concentrations, or where it is modified by external sources

of point defects (e.g. surface reactions), stress, or crystallographic imperfections, these plots are not applicable. Instead of theoretical plots, experimental ones should be used.

Another popular method of diffusion characterization is dopant profiling using secondary-ion mass spectroscopy (SIMS) for the concentrations of chemical dopants. It is based on ion sputtering of doped layers and allows depth profiling of the atomic composition. This technique is frequently supplemented by carrier analyses obtained by spreading resistance profiling (SRP). Here, a doped layer is beveled to allow resistance measurements from the Si surface to the p–n junction and subsequent conversion of resistance to carrier concentration. Large discrepancies between SIMS and SRP measurements are useful in the determination of poor dopant activation, which can indicate process-induced defects and/or poor dopant activation.

Dopant profiling is especially important in the characterization of extrinsic diffusion processes where neither erfc nor Gaussian functions are appropriate. A diffusion coefficient at any point of a nonideal profile obtained by SIMS can be calculated using the Boltzmann–Matano method (5). That allows for diffusivity determination as a function of dopant concentration, thus revealing anomalies of the specific diffusion conditions. The usefulness of this technique is restricted by the limited efficiency dopant sources used in some prediffusion processes that decrease the surface concentration below the solid solubility in Si. This limitation does not arise from redistribution processes, since the total concentrations are known despite the decreasing surface concentration during the process.

BIBLIOGRAPHY

1. W. Zagozdzon-Wosik et al., Formation of shallow junctions during rapid thermal diffusion from electron-beam deposited boron sources, *J. Electrochem. Soc.,* **9**: 2981–2989, 1996.
2. P. M. Fahey, P. B. Griffin, and J. D. Plummer, Point defect and dopant diffusion in silicon, *Rev. Mod. Phys.,* **61**: 289–384, 1989.
3. C. Claeys and J. Vanhellemont, Defects in crystalline silicon, in J. F. A. Nijs (ed.), *Advanced Silicon and Semiconducting Silicon-alloy Based Materials and Devices,* Bristol: Inst. Phys., 1994, pp. 35–102.
4. D. Nobili, Equilibrium carrier density and solubility of silicon dopant, in H. R. Huff, K. G. Barraclough, and J.-I. Chikawa (eds.), *Semiconductor Silicon,* Pennington, NJ: Electrochem. Soc., 1990, pp. 550–564.
5. W. R. Runyan and K. E. Bean, *Semiconductor Integrated Circuit Processing Technology,* Reading, MA: Addison-Wesley, 1990.
6. M. Ono et al., *IEEE Trans. Electron Devices,* **42**: 1822–1830, 1995.
7. *PDS*® Phosphorus, Arsenic, Boron Planar Diffusion Source, Tech. Data, Standard Oil Engineering Ceramic Division, Carborundum Products, Amherst, NY, 1997.
8. Y. Sato, K. Imai, and N. Yabumoto, *J. Electrochem. Soc.,* **144**: 2548–2551, 1997.
9. K. V. Ravi, *Imperfections and Impurities in Semiconductor Silicon,* New York: Wiley-Interscience, 1981.
10. S. M. Hu, Vacancies and self-interstitials in silicon, in W. M. Bullis, U. Gosele, and F. Shimura (eds.), *Defects in Silicon II,* Pennington, NJ: Electrochem. Soc., 1991, Vol. 91-9, pp. 211–236.
11. R. B. Fair, Diffusion and ion implantation in silicon, in E. McGuire (ed.), *Semiconductor Materials and Process Technology Handbook for Very Large Integration (VLSI) and Ultra Large Scale Integration (ULSI),* Park Ridge, NJ: Noyes Publications, 1988, pp. 455–540.
12. S. M. Hu, *J. Appl. Phys.,* **51**: 3666–3671, 1980.
13. K. Nishi and D. A. Antoniadis, *J. Appl. Phys.,* **59**: 1117–1124, 1986.
14. G. D. Watkins, J. R. Troxell, and A. P. Chatterjee, *Def. Radiat. Eff. Semicond.,* **46**: 16, 1979.
15. S. Dannefaer, P. Masher, and D. Kerr, *Phys. Rev. Lett.,* **56**: 2195, 1986.
16. D. J. Roth and J. D. Plummer, *J. Electrochem. Soc.,* **141** (4): 1074–1081, 1994.
17. A. Seeger and K. P. Chick, *Phys. Status Solidi,* **29**: 455, 1968.
18. W. B. Richardson and B. J. Mudvaney, *J. Appl. Phys.,* **65**: 2243–2247, 1989.
19. R. B. Fair, Concentration profiles of diffused dopants in silicon, in F. F. Y. Wang (ed.), *Impurity Doping Processes in Silicon: Materials Processing—Theory and Practice,* Amsterdam: North-Holland, 1981, pp. 317–442.
20. N. E. B. Cowern, *Appl. Phys. Lett.,* **54**, 703–705, 1989.
21. Y. Hayafugi, K. Kajiwara, and S. Usui, *J. Appl. Phys.,* 8639–8646, 1982.
22. P. A. Stolk et al., *J. Appl. Phys.,* **81**: 6031–6050, 1997.
23. R. Scholz et al., *Appl. Phys. Lett.,* **72**: 200–202, 1998.
24. P. M. Fahey et al., *Appl. Phys. Lett.,* **46**: 784–786, 1985.
25. H.-J. Grossmann et al., *Appl. Phys. Lett.,* **71** (26): 3862–3864, 1997.
26. J. D. Plummer and S. T. Pantelides (eds.), *Process Physics and Modeling in Semiconductor Technology, Diffusion and Thermal Processing,* Pennington, NJ: Electrochem. Soc., 1991, pp. 175–384.
27. M. Orlowski, Challenges for process modeling and simulation in the 90's—An industrial perspective, in W. Fichtne (ed.), *Simulation of Semiconductor Devices and Processes,* Zurich, Switzerland: D. Aemmer, 1991, Vol. 4, pp. 3–22.
28. R. B. Fair and J. C. C. Tsai, *J. Electrochem. Soc.,* **124** (7): 1107–1118, 1977.
29. P. Fahey, R. W. Dutton, and S. M. Hu, *Appl. Phys. Lett.,* **44** (8): 777–779, 1984.
30. L. C. Kimerling, Defect control in silicon processing, in H. R. Huff, K. G. Barraclough, and J.-I. Chikawa (eds.), *Semiconductor Silicon 1990,* H. R. Huff, K. G. Barraclough, and J.-I. Chikawa (eds.), Pennington, NJ: Electrochem. Soc., 1990, pp. 117–130B.
31. C. G. Van de Walle, Hydrogen in crystalline semiconductors, in S. T. Pantelides (ed.), *Deep Centers in Semiconductors, A State of the Art Approach,* New York: Gordon and Breach, 1992, pp. 899–926.
32. A. F. Willoughby, Double-diffusion processes in silicon, in F. F. Y. Wang (ed.), *Impurity Doping Processes in Silicon, Materials Processing—Theory and Practice,* Amsterdam: North-Holland, 1981, pp. 3–53.
33. F. Gaiseanu and W. Schroter, *J. Electrochem. Soc.,* **143**, 361–362, 1996.
34. M. A. Berding et al., *Appl. Phys. Lett.,* **72** (12): 1492–1494, 1998.
35. S. T. Ahn et al., *Appl. Phys. Lett.,* **53**: 1593–1505, 1988.
36. K. Nishi, K. Sakamoto, and J. Ueda, *J. Appl. Phys.,* **59**: 4177–4179, 1986.
37. B. E. Deal, The thermal oxidation of silicon and other semiconductor materials, in E. McGuire (ed.), *Semiconductor Materials and Process Technology Handbook for Very Large Integration (VLSI) and Ultra Scale Integration (ULSI),* Park Ridge, NJ: Noyes Publications, 1988, pp. 46–79.
38. T. Y. Tan and U. Gosele, *Appl. Phys. Lett.,* **40**: 616, 1982.

39. S. Mizuo and H. Higuchi, Investigation of point defects in Si by impurity diffusion, *Mater. Res. Soc. Symp. Proc.,* pp. 125–130, 1985.
40. N. K. Chen and C. Lee, *J. Electrochem. Soc.,* **143**: 352–355, 1996.
41. P. Fahey and P. Griffin, Investigation of the mechanism of Si self-interstitial injection from nitridation of SiO_2 films, in H. R. Huff, K. G. Barraclough, and J.-I. Chikawa (eds.), *Semiconductor Silicon 1990,* Pennington, NJ: Electrochem. Soc., 1990, pp. 486–495.
42. S. A. Abbasi and F. Rahman, *J. Electrochem. Soc.,* **142**: 3928–3932, 1995.
43. R. Francis and P. S. Dobson, *J. Appl. Phys.,* **50**: 280, 1979.
44. T. Y. Tan and B. J. Ginsgerg, *Appl. Phys. Lett.,* **42**: 448, 1983.
45. M. M. Mandurah et al., *J. Appl. Phys.,* **51**: 5755–5762, 1980.
46. K. Suzuki et al., *J. Electrochem. Soc.,* **138**, 2201–2205, 1991; **142**: 2786–2789, 1995.
47. A. H. Van Ommen, *Solid State Phenomena,* **182**: 133–152, 1988.
48. R. B. Fair, *J. Electrochem. Soc.,* **144**: 708–717, 1997.
49. M. Susa et al., *J. Electrochem. Soc.,* **144**: 2552–2558, 1997.
50. Y. Sato et al., *J. Electrochem. Soc.,* **142**: 653–660, 660–663, 1995.
51. S. P. Murarka, *Silicides for VLSI Applications,* Orlando, FL: Academic Press, 1983.
52. P. Fahley and M. Wittmer, *Mater. Res. Soc. Symp. Proc.,* **163**: 529–534, 1989.
53. S. M. Hu, *Appl. Phys. Lett.,* **51**: 308–310, 1987.
54. H. Jiang et al., *J. Electrochem. Soc.,* **139** (Part I): 196–206, (Part II): 206–211, (Part III): 211–218, 1992.
55. A. Mitwalsky et al., Metal–dopant compound formation in $TiSi_2$ studied by transmission and scanning electron microscopy, in H. R. Huff, K. G. Barraclough, and J.-I. Chikawa (eds.), *Semiconductor Silicon 1990,* Pennington, NJ: Electrochem. Soc., 1990, pp. 876–886.
56. W. Zagozdzon-Wosik et al., Silicide contacts to shallow junctions produced via rapid thermal processing from electron beam deposited dopant sources, in R. Fair, et al. (eds.), *Proc. 4th Int. Conf. on Rapid Thermal Processing, RTP'96,* 1996, pp. 411–416.
57. S. M. Hu, Stress-related problems in silicon technology, in J. D. Plummer and S. T. Pantelides (eds.), *Process Physics and Modeling in Semiconductor Technology, Diffusion and Thermal Processing,* Pennington, NJ: Electrochem. Soc., 1991, pp. 548–582.
58. V. Rao and W. Zagozdzon-Wosik, Stress effects in 2D arsenic diffusion in silicon, in *Mater. Res. Soc. Symp. Proc.,* 1995, pp. 345–350.

WANDA ZAGOZDZON-WOSIK
University of Houston